Numerical methods for axisymmetric and 3D nonlinear beams

Gianmarco F. Pinton and Gregg E. Trahey
Department of Biomedical Engineering
Duke University, Durham, NC 27708

***Abstract*— Time domain algorithms that solve the Khokhlov–Zabolotzskaya–Kuznetsov (KZK) equation are described and implemented. This equation represents the propagation of finite amplitude sound beams in a homogenous thermoviscous fluid for axisymmetric and fully three dimensional geometries. In the numerical solution each of the terms is considered separately and the numerical methods are compared with known solutions. First and second order operator splitting are used to combine the separate terms in the KZK equation and their convergence is examined.**

I. Introduction

Linear theory provides a suitable approximation for small amplitude waves and short propagation lengths. Although in many cases this approximation is sufficient, a higher order description is necessary where large amplitudes or long propagation lengths and small attenuation is involved. Examples of such waves are beams with an amplitude large enough to produce shock waves, such as those used in therapeutic ultrasound for lithotripsy[1] or for harmonic imaging[2].

Several numerical methods have been implemented to solve equations that describe nonlinear wave propagation[3–6]. Although these methods are useful, significant challenges remain in modeling certain pulses and geometries at the initial condition surface.

Lee *et al.*[4] solved the axisymmetric Khokhlov–Zabolotzskaya–Kuznetsov (KZK) equation in the time domain using implicit centered differences and the Crank-Nicolson scheme[7] for both the integral form of the diffraction operator and the absorption, and a distorted time solution for the nonlinearity. The propagation step was combined for pulsed unfocused waves using a first order operator split. Yang directly extended these methods to three dimensions[6]. Here, in addition to these methods, we consider solutions of the KZK equation in axisymmetric and cartesian coordinates with a number of different numerical techniques. The diffraction is solved using the differential form of the operator for pulsed unfocused waves and focused plane waves. The nonlinearity is solved with the Lax-Friedrichs and Lax-Wendroff methods[7]. These are applied separately to each term in the equations and compared to known solutions for pulsed unfocused waves and continuous focused waves or to frequency domain solutions. Then the combined effect for first and second order operator splitting are determined and compared.

II. Basic Equations

The nonlinear parabolic KZK wave equation describes the effects of diffraction, absorption, and nonlinearity. Its axisymmetric form in terms of pressure can be written as[8]

$$\frac{\partial^2 p}{\partial z \partial t'} = \frac{c_0}{2}\left(\frac{\partial^2 p}{\partial r^2} + \frac{1}{r}\frac{\partial p}{\partial r}\right) + \frac{\delta}{2c_0^3}\frac{\partial^3 p}{\partial t'^3} + \frac{\beta}{2\rho_0 c_0^3}\frac{\partial^2 p^2}{\partial t'^2} \quad (1)$$

where $t' = t - z/c_0$ is the retarded time, z is the direction of propagation. The first term on the right hand side represents diffraction, with c_0 as the small signal speed of sound. The second term accounts for thermoviscous attenuation with δ as the diffusivity parameter. Nonlinearity is described in the third term with $\beta = 1 + B/2A$ as the coefficient of nonlinearity and ρ_0 as the ambient fluid density. The quotient B/A is derived from the expansion of the equation of state for the fluid.

Equation 1, describes directional sound beams[5, 9] and is valid when $ka \gg 1$, where k is the wave number and a is the characteristic width of the source. For focused sources Eq. 1 can be nondimensionalized as[9, 10]:

$$\frac{\partial^2 P}{\partial \sigma \partial \tau} = \frac{1}{4G}\left(\frac{\partial^2 P}{\partial R^2} + \frac{1}{R}\frac{\partial P}{\partial R}\right) + A\frac{\partial^3 P}{\partial \tau^3} + NP\frac{\partial^2 P}{\partial \tau^2} \quad (2)$$

with scaling,

$$P = p/p_p, \quad \sigma = z/d, \quad R = r/a, \quad \tau = \omega_0 t' \quad (3)$$

The dimensionless parameters in Eq. 2 are

$$G = d/\bar{z}, \quad N = d/\bar{z}, \quad A = \alpha_0 \bar{z} \quad (4)$$

where $\bar{z} = \rho_0 c_0^3/\beta p_p \omega_0$ is the plane wave shock formation distance for the pressure p_p, $\alpha_0 = \delta\omega_0^2/2c_0^3$ is the thermoviscous attenuation coefficient at a frequency w_0, and d is the characteristic focusing length. The parameters G, N, A, respectively represent the small-signal focusing gain, nonlinearity, and thermoviscous absorption.

Equation 1 can be similarly nondimesionalized for unfocused sources. These equations are easily extended to 3D by transforming the transverse Laplacian to cartesian coordinates.

III. Operator Splitting

Operator splitting applies numerical techniques to each of the terms in the equation independently over a propagation step[4, 7]. The KZK equation can be rewritten as

$$\frac{\partial P}{\partial \sigma} = \mathcal{L}_D(P) + \mathcal{L}_A(P) + \mathcal{L}_N(P) \quad (5)$$

where $\mathcal{L}_D, \mathcal{L}_A$, and $\mathcal{L}_N$ are the operators for diffraction, absorption, and nonlinearity. A first order operator splitting scheme applies the numerical methods sequentially at each propagation step thus approximating the solution:

$$P = S_{\mathcal{L}_N \Delta\sigma} \circ S_{\mathcal{L}_A \Delta\sigma} \circ S_{\mathcal{L}_D \Delta\sigma}(P_0) + O(\Delta\sigma^2) \quad (6)$$

where P_0 is the initial condition and $\Delta\sigma$ is the step size in the direction of propagation. A second order operator splitting scheme can be constructed by solving for a half step with one operator, then using that solution to propagate a full step in another operator, and finally completing the calculation by a half step in the first operator, i.e.:

$$P = S_{\mathcal{L}_{D+A} \Delta\sigma/2} \circ S_{\mathcal{L}_N \Delta\sigma} \circ S_{\mathcal{L}_{D+A} \Delta\sigma/2}(P_0) + O(\Delta\sigma^3) \quad (7)$$

where the diffraction and absorption operator is combined.

IV. Diffraction

Diffraction was determined by using the integral and differential forms of the operator. In the first case the equation

$$\frac{\partial P}{\partial \sigma} = \mathcal{L}_D(P) = \frac{1}{4G} \int_{-\infty}^{\tau} \left(\frac{\partial^2 P}{\partial R^2} + \frac{1}{R} \frac{\partial P}{\partial R} \right) d\tau' \quad (8)$$

was solved as described by Lee[4] using finite difference approximations for the derivatives and the trapezoidal rule for the integral. Implicit centered differences and the Crank-Nicolson methods were used. Since the Crank-Nicolson scheme is not monotone[7] a numerical smoothing step was added to prevent spurious numerical oscillations.

The diffraction step was also solved directly in its differential form as shown in Eq. 2 with both implicit centered differences and Crank-Nicolson schemes applied to the entire system thus obviating the need for an integration step. In order to keep the entire method second order the first order temporal derivative was differenced to second order:

$$\frac{\partial P}{\partial \tau} \doteq \frac{\frac{3}{2} P_i - 2P_{i-1} + P_{i-2}}{\Delta\tau} \quad (9)$$

where the index i references τ.

A. Focused Equations

The well-known solution to the source condition

$$P_0 = e^{-R^2} sin(\tau + GR^2), \quad (\sigma = 0) \quad (10)$$

is provided by the linear theory of diffracting beams and can be found in[10].

Figure 1 compares the numerical solutions to the analytical solution for the initial conditions shown in Eq. 10. The left plot shows an axial slice $(R = 0)$ of the nondimensionalized pressure with respect to retarded time, τ at the focal point $(\sigma = 1)$. Methods that use the integral form of the diffraction operator exhibit more amplitude error than their counterparts for the differential form for nondimensional depths greater than 0.7. The accumulation of phase error with propagation is more pronounced for the integral method than it is for the fully differenced method. Note that the stair-step patterns are due to the discrete nature of the signals being compared.

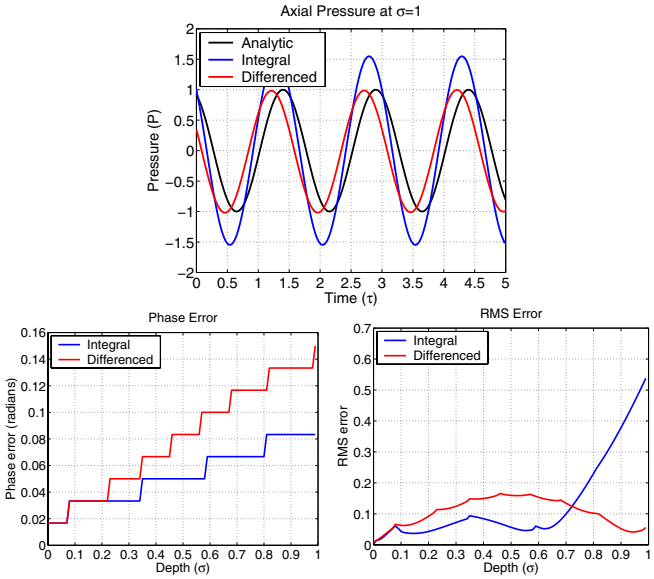

Fig. 1. Axisymmetric coordinates. Axial (R=0) nondimensionalized pressure for a focused continuous wave (see Eq. 10) after propagating a distance of $\sigma = 1$ (top). The phase error is shown between the analytical solution, the integral method (Lee), and the differenced method (Pinton) as a function of depth (bottom left). The root mean square error assuming no phase error (bottom right).

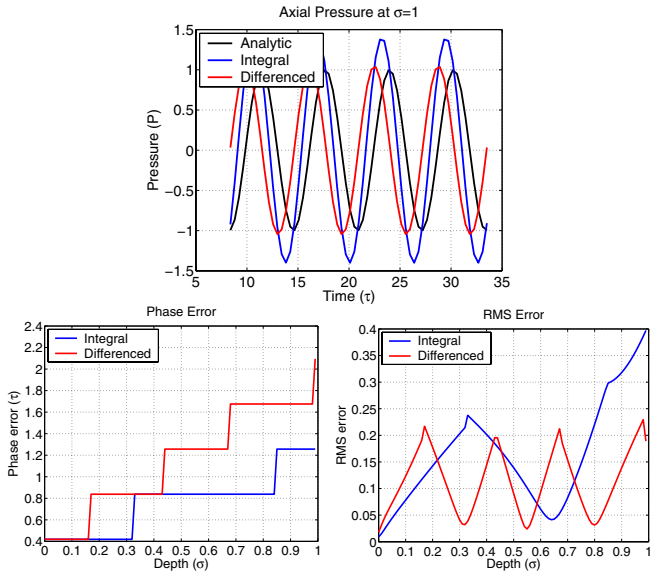

Fig. 2. Cartesian coordinates. Axial (R=0) nondimensionalized pressure for a focused continuous wave (see Eq. 10) after propagating a distance of $\sigma = 1$ (top). The phase error is shown between the analytical solution, the integral method (Yang) and the differenced method (Pinton) as a function of depth (bottom left). The root mean square error assuming no phase error (bottom right).

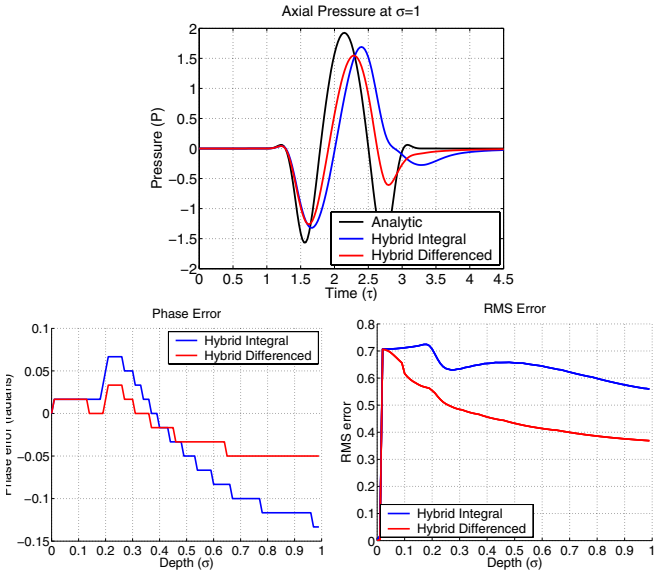

Fig. 3. Axisymmetric coordinates. Axial (R=0) nondimensionalized pressure for a focused continuous wave (see Eq. 11) after propagating a distance of $\sigma = 1$. (top). The phase error is shown between the analytical solution, the integral method (Lee), and the differenced method (Pinton) as a function of depth (bottom left). The root mean square error assuming no phase error (bottom right).

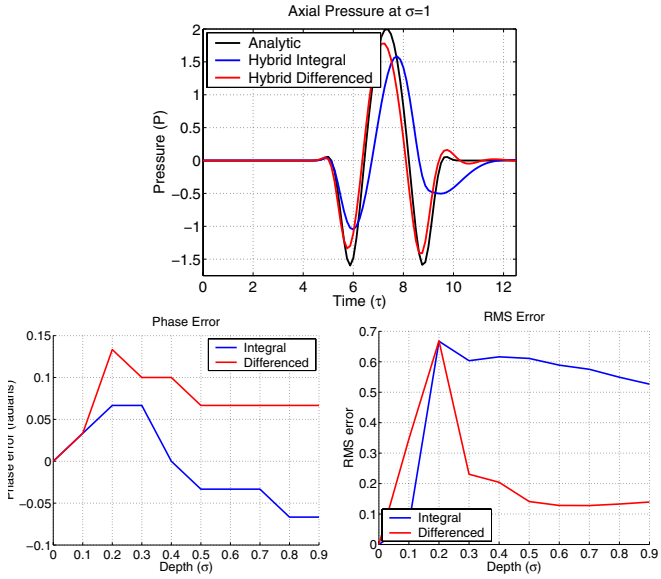

Fig. 4. Cartesian coordinates. Axial (R=0) nondimensionalized pressure for a focused continuous wave (see Eq. 11) after propagating a distance of $\sigma = 1$. (top). The phase error is shown between the analytical solution, the integral method (Yang) and the differenced method (Pinton) as a function of depth (bottom left). The root mean square error assuming no phase error (bottom right).

Figure 2 performs the same comparison as 1 but in 3D. The numerical methods exhibit almost identical charactersitcs though the discretization is more apparent due to the smaller grid size.

B. Unfocused Equations

The initial condition for the unfocused equations represent a circular source mounted on a rigid baffle. The pulse is given by:

$$f(\tau + R^2) = \exp\left[-\left(\frac{2(\tau + R^2)}{\omega_0 T}\right)^{2m}\right] \sin(\tau + R^2) \quad (11)$$

The solution to this equation can be found in [4].

Figure 3 compares the numerical solutions to the analytical solution for the initial conditions shown in Eq. 11. The left plot shows an axial slice $(R = 0)$ of the nondimensionalized pressure with respect to retarded time, τ at the focal point $(\sigma = 1)$. Methods that use the fully differenced form have less phase and less rms error across the depth range. Similar results are obtained for the 3D case shown in 4.

V. Nonlinearity

The nonlinear step can be performed as described by Lee[4] by interpolating the pressure on a distorted time. In addition to this method, the nonlinearity was solved using a first order Lax-Friedrichs scheme and a second order Lax-Wendroff scheme. For the equation

$$\frac{\partial P}{\partial \sigma} = NP\frac{\partial P}{\partial \tau} \quad (12)$$

The Lax-Friedrichs scheme on a uniform axial and temporal grid can be written as

$$P_{i+1/2}^{n+1/2} = \frac{P_i^n + P_{i+1}^n}{2} - \frac{N\Delta\sigma}{2\Delta\tau}[(P_{i+1}^n)^2 - (P_i^n)^2] \quad (13)$$

$$P_i^{n+1} = \frac{P_{i-1/2}^{n+1/2} + P_{i+1/2}^{n+1/2}}{2} - \frac{N\Delta\sigma}{2\Delta\tau}[(P_{i+1/2}^{n+1/2})^2 - (P_{i-1/2}^{n+1/2})^2] \quad (14)$$

The Richtmeyer two-step Lax-Wendroff scheme can be expressed as

$$P_{i+1/2}^{n+1/2} = \frac{P_i^n + P_{i+1}^n}{2} - \frac{N\Delta\sigma}{2\Delta\tau}[(P_{i+1}^n)^2 - (P_i^n)^2] \quad (15)$$

$$P_i^{n+1} = P_i^n - \frac{N\Delta\sigma}{\Delta\tau}[(P_{i+1/2}^{n+1/2})^2 - (P_{i-1/2}^{n+1/2})^2] \quad (16)$$

The nonlinear and absorption operators together form the well-studied Burgers' equation which can be solved numerically using methods for scalar hyperbolic conservation laws[7] or frequency domain techniques [9]. By assuming a periodic plane wave solution the equation

$$\frac{\partial P}{\partial \sigma} = A\frac{\partial^2 P}{\partial \tau^2} + NP\frac{\partial P}{\partial \tau} \quad (17)$$

can be approximated by

$$\frac{dP_n}{d\sigma} = -n^2 AP_n + iN\frac{n}{4}\left(\sum_{m=1}^{n-1} P_m P_{n-m} + 2\sum_{m=n+1}^{M} P_m P_{m-n}^*\right) \quad (18)$$

where M is the number of harmonics retained which also corresponds to the size of the dense system of coupled ordinary differential equations required to solve Burgers' equation. These ODE's can be solved with standard methods such as

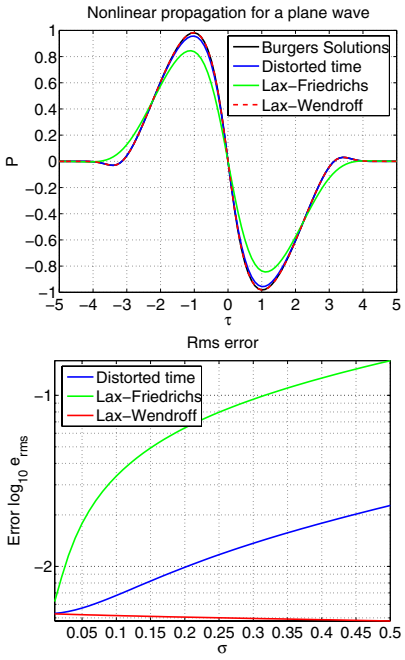

Fig. 5. Nonlinear propagation. Propagated pulse (top) and the rms error with propagation depth (bottom). The known numerical solution of Burgers' equation is compared with the distorted time method (Lee) and nonlinear hyperbolic partial differential equation finite difference methods. The initial conditions for the pulsed plane wave are given in Eq. 11 with $\omega_0 T = 6, m = 3, R = 0$ and $N = 1, A = 0$.

fourth order Runge-Kutta. The first summation in Eq. 18 represents the sum-frequency generation and the second summation difference frequency generation.

Figure 5 compares the frequency domain pulsed plane wave solution with the previously described time domain numerical techniques. On the top plot the nonlinearly propagated pulse is shown using the previously described methods. The solutions are propagated to a value of $\sigma = 0.5$ with a nonlinearity $N = 1$. The top shows the pressure waveform and the bottom plot shows the log of the root mean square error. The Lax-Friedrichs scheme and the distorted time solutions have an error that increases with propagation whereas the Lax-Wendroff scheme has a constant, if not slightly decreasing error.

VI. Convergence

There is no analytical solution to the KZK equation but the convergence of the combined methods can be examined by comparing solutions for a given $\Delta\sigma$ with that obtained with a highly refined grid. Figure VI shows the root mean square error as a function of step size with a reference of $\Delta\sigma = 10^{-4}$. These curves were obtained for a first and second order operator split on the integral form of the Crank-Nicolson scheme with the Lax-Wendroff scheme for the nonlinearity and a focused plane wave initial condition. The other differencing schemes have similar convergence plots.

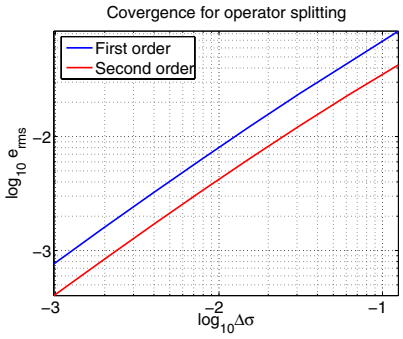

Fig. 6. Convergence of first and second order operator splitting methods. The reference step size is $\Delta\sigma = 10^{-4}$

VII. Summary

Several time domain algorithms to solve the KZK equation in axisymmetric and cartesian coordinates were described and implemented. Results were compared with solutions for continuous focused waves and pulsed unfocused waves. The integral formulation had less phase error for narrowband pulses. At large nondimensional depths the differential formulation had less rms error. Time domain techniques are perhaps better suited to model narroband pulses. In this case the differential formulation had less phase and less rms error for all depths. Methods for the nonlinear step were analyzed with reference to the frequency domain solution. The Lax-Wendroff scheme had the least amount of error. Second order operator splitting had a faster convergence to the solution though the slope was the same as first order splitting.

References

[1] M. A. Averkiou, Y. S. Lee, and M. F. Hamilton, "Self-demodulation of amplitude- and frequency-modulated pulses in a thermoviscous fluid," *Journal of the Acoustical Society of America*, vol. 94, pp. 2876–2883, 1993.

[2] T. Christopher, "Finite amplitude distortion-based inhomogeneous pulse echo ultrasonic imaging," *IEEE Transactions on Ultrasonics Ferroelectrics and Frequency Control*, vol. 44, no. 1, pp. 125–139, 1997.

[3] P. T. Christopher and K. J. Parker, "New approaches to nonlinear diffractive field propagation," *Journal of the Acoustical Society of America*, vol. 90, no. 1, pp. 488–499, Jul 1991.

[4] Y.-S. Lee and M. F. Hamilton, "Time-domain modeling of pulsed finite-amplitude sound beams," *Journal of the Acoustical Society of America*, vol. 97, no. 2, pp. 906–917, February 1995.

[5] M. A. Averkiou and M. F. Hamilton, "Nonlinear distortion of short pulses radiated by plane and focused circular pistons," *Journal of the Acoustical Society of America*, vol. 102, no. 5, pp. 2539–2548, 1997.

[6] X. Yang and R. O. Cleveland, "Time domain simulation of nonlinear acoustic beams generated by rectangular pistons with application to harmonic imaging," *J. Acoust. Soc. Am.*, vol. 117, no. 1, pp. 113–123, January 2005.

[7] J. A. Trangenstein, *Numerical Solution of Partial Differential Equations (in preparation)*.

[8] N. S. Bakhvalov, Y. M. Zhileikin, and E. A. Zabolotskaya, *Nonlinear Theory of Sound Beams*. American Institute of Physics, New York, 1987.

[9] M. F. Hamilton and D. T. Blackstock, *Nonlinear Acoustics*. Academic Press, San Diego, 1997.

[10] M. F. Hamilton, V. A. Khokhlova, and O. V. Rudenko, "Analytical method for describing the paraxial region of finite amplitude sound beams," *Journal of the Acoustical Society of America*, vol. 101, no. 3, pp. 1298–1308, March 1997.